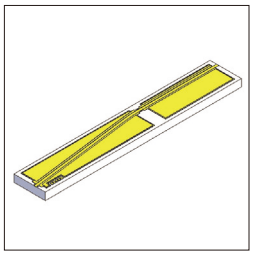

400 mW-Class 1.3 µm High-Power Semiconductor Laser for CPO Application

Konosuke AOYAMA*, Daisuke INOUE, Naoki FUJIWARA, Harold KAMISUGI, and Daisei SHOJI

The growing demand for generative AI and high-performance computing has increased the importance of high-speed, energy-efficient communications in data centers, leading to an increased focus on co-packaged optics (CPO). The external laser sources (ELSs), a component of CPO, require high optical output power of several hundred mW and low power consumption with power conversion efficiency greater than 20%. This paper discusses the integration of a wide stripe waveguide semiconductor optical amplifier (SOA) into a 1.3 µm high-power semiconductor laser for CPO. By using an electrically isolated structure for each element, we have optimized the power distribution to achieve over 400 mW output power and 25% power conversion efficiency at a temperature of 45°C.

Keywords: semiconductor lasers, semiconductor optical amplifiers, optical communications, high-power lasers

1. Introduction

With the recent proliferation of generative AI and high-performance computing, there is a significant increase in demand for short-distance fiber optic communication, such as within data centers for distances of less than 1 km. To address this increasing demand for short-distance fiber optic communication, it is particularly important to increase the speed and reduce the power consumption of communication systems. To this end, the industry is promoting the introduction of Co-Packaged Optics (CPO) technology, which compactly houses both the electrical integrated circuit and the optical transceiver system in the same package.[1],[2]

CPO technology can shorten the electrical wiring between the optical transceiver system and the electrical integrated circuit, enabling faster communication and reducing power loss. On the other hand, when using a combination of silicon photonics and lasers, which perform signal processing within the optical transceiver system, the semiconductor laser requires a high optical output of over 100 mW to compensate for the optical loss that occurs. To keep the overall system power consumption low, it is necessary to maintain a high power conversion efficiency (PCE) of over 20% even when operating at high optical output.[3]

With the introduction of CPO for data center communications, research is also being actively conducted into high-power laser sources in the 1.3 µm band, which are external laser sources (ELSs). Structures using long laser cavity and integration of distributed feedback laser diodes (DFB-LDs)*1 and semiconductor optical amplifiers (SOAs)*2 have been reported, with laser sources exceeding 100 mW optical output.[4]-[6]

In the midst of these trends, we have achieved a high-efficiency semiconductor laser source with a PCE of 25% and an optical output of over 400 mW at a stage temperature of 45°C. This was achieved by introducing a wide stripe structure used in high-output LDs, such as processing LDs and fiber laser excitation LDs, and by optimizing the input power for each region using electrical component separation to improve the PCE.

2. Device Structure

Attaining high laser output is considerably effective with the wide-stripe waveguide structure. However, it is challenging to achieve single-mode oscillation with the laser cavity of a wide-stripe waveguide structure; therefore, it is inappropriate for applications like optical communication that demand high coherence. Therefore, as represented in Fig. 1, we balanced high output with coherence by forming a device with the integrated structure of both a DFB-LD section, which satisfies the single-mode propagation condition, and a SOA section, which amplifies the DFB-LD light in the wide-stripe waveguide.

The waveguide width of the SOA section of this device is set to 7.2 µm, and the total length of the device is 2 mm. The wide waveguide width of this SOA section allows for a reduction in photon density, in turn enabling the suppression of gain saturation. It also allows a reduction in heat generation due to lower electrical resistance, and through the expansion of the heat dissipation route, achieving improved thermal resistance results in a decrease in active layers temperature during operation, thereby allowing an increase in optical output.

The DFB-LD and SOA sections are coupled through the active layers by a taper waveguide structure. The DFB-LD section, which easily reaches optical output satu-

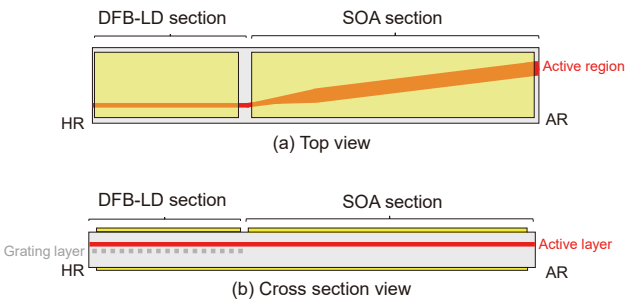

Fig. 1. Schematic of device structure
(a) Plan view (b) Waveguide cross section

ration, operates at low current for the purpose of generating coherent light as a seed light source. By increasing the SOA current correspondingly, the whole device can achieve a high PCE along with coherence.

The output facet of the SOA section is treated with an anti-reflection (AR) coat, and the end facet of the DFB-LD section is treated with a high-reflection (HR) coat. Since the SOA is placed on the emission side of this device structure, there is a risk of laser oscillation occurring with the SOA part as a resonator if reflection occurs at the output facet. Therefore, by adopting a diagonal waveguide structure with an angle to the output facet, output facet reflection is suppressed[8] and side-mode suppression ratio (SMSR)*3 degradation restrained.

3. Device Characteristics

3-1 Emission characteristics

In evaluating the device characteristics, we tested them in a Chip-on-submount (CoS) where the LD chip is installed on an AlN heat sink. The device temperature T_c is defined as the stage temperature where the CoS is installed. Figure 2 displays the temperature dependence of light output, where P_o denotes the light output from the SOA section, and I_{SOA} and I_{DFB} illustrate the injection currents of the SOA and DFB-LD sections, respectively. In this instance, an injection I_{DFB} current of 250 mA is targeted at the DFB-LD section with a threshold current of about 17 mA at 25°C.

The maximum light outputs achieved at T_c: 25°C, 45°C, and 65°C are 600 mW, 450 mW, and 320 mW each, confirming the successful generation of high outputs using a wide-stripe SOA section. Envisioning actual operating conditions and using 0.7 times the SOA current values at each maximum output as the operating current, operating light outputs of 530 mW (I_{SOA} =1.05 A), 400 mW (I_{SOA} =0.88 A), and 280 mW (I_{SOA} =0.78 A) were achieved at T_c: 25°C, 45°C and 65°C, respectively, securing sufficient light outputs as ELSs for CPO applications.

The PCE of our device, having independent SOA and DFB-LD sections, is given by:

$$\mathrm{PCE} = \frac{P_o}{I_{SOA} \cdot V_{SOA} + I_{DFB} \cdot V_{DFB}} \quad \cdots\cdots (1)$$

Where, V_{SOA} and V_{DFB} denote applied voltages to the SOA and DFB-LD sections, respectively. Figure 3 shows the temperature dependence of PCE on the light output. The maximum PCEs at T_c: 25°C, 45°C, 65°C are 33%, 28%, and 22% respectively, and 28%, 25%, and 21% respectively under actual operating conditions, confirming highly efficient emission characteristics.

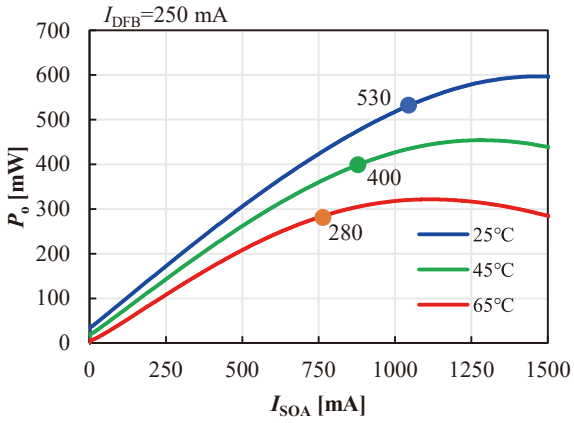

Fig. 2. Device temperature dependence of optical output

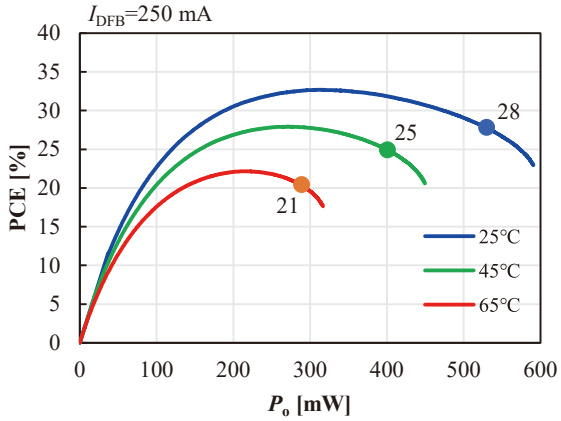

Fig. 3. Device temperature dependence of PCE

3-2 Oscillation spectrum

In CPO applications, oscillation spectra demand single-mode and high SMSR. Specifically, in integrated SOA device structures, SMSR degradation due to amplified spontaneous emission (ASE)*4 noise occurring in the SOA or output facet reflection has been reported when the light output intensity of the DFB-LD is not strong enough.[9] Therefore, necessitating confirmation whether optical communication applications can be adopted through the evaluation of oscillation spectra and whether the SOA is operating in a resonant manner.

We first confirm the emission characteristics of the DFB-LD section alone, without integrated SOA. Figure 4 shows the emission characteristics in the structure of the DFB-LD section alone. At this time, the output facet of the DFB-LD section is provided with an AR coat. Like Section 3-1, if the operating current of the DFB-LD is 250 mA, the light outputs obtained at T_c: 25°C, 45°C, 65°C are 124 mW, 113 mW, and 90 mW respectively. Compared to the actual operating conditions in Section 3-1, the SOA gain in the SOA integrated structure was 6.3 dB, 5.5 dB, and 4.9 dB at T_c: 25°C, 45°C, 65°C, all indicating a low amplification rate.

Given that the small signal gain of SOAs is generally 20dB or more and the saturated optical output is around 10 mW, SOA can be discerned as operating in the gain satura-

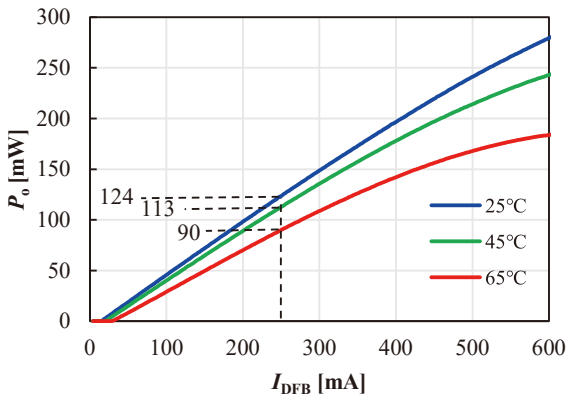

Fig. 4. Current and optical output characteristics of DFB-LD section alone

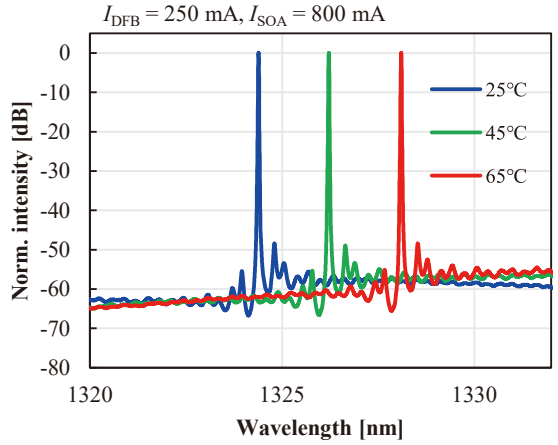

Fig. 5. Device temperature dependence of oscillation spectrum

tion state based on its low amplification rate.[8] Since it is in gain saturation state, most of the carriers injected into the SOA are consumed by the induced release, enabling operation conditions to suppress the generation of ASE noise. The temperature dependence of the oscillation spectrum measured at I_{SOA} = 800 mA is shown in Fig. 5. Single-mode oscillation can be confirmed under all measured conditions, confirming that only the 0th-mode laser light of the DFB-LD is amplified in the SOA section in line with the concept of device design.

In addition, a stable SMSR of over 45 dB is obtained, and since no spectral peak called the external cavity mode[10] is occurring, it can be confirmed that it is not being influenced by the ASE of SOA or the reflection of the SOA end, ensuring sufficient coherence for optical communication applications. Furthermore, as ELSs for CPO, the oscillation spectral stability is also required. High output lasers and long cavity lasers are known to easily induce mode hopping due to spatial hole burning.[11] Mode hopping is the phenomenon where the oscillation spectrum jumps to another adjacent wavelength, which can also lead to multimode oscillation. Furthermore, discontinuous changes called kinks also occur in the light output at the same time, which becomes problematic when controlling within an optical communication system.

Contrarily, since our device structure mainly uses the SOA section to achieve high output, the optical density of the DFB-LD section is relatively low, resulting in a structure that is less likely to cause spatial hole burning. The occurrence of mode hopping can be confirmed by seeing continuous changes in the oscillation frequency through a wide range of current sweeps as it occurs when the internal electric field strength of the laser changes due to changes in the injection current. Figure 6 shows the change in the oscillation spectrum peak when the I_{DFB} is swept from 52.5 to 350 mA and the I_{SOA} is swept from 0 to 1500 mA at T_c: 45°C. The oscillation spectrum during each current sweep ends with regular intervals of oscillation, confirming no mode hopping occurrences, and a stable oscillation spectrum can be obtained.

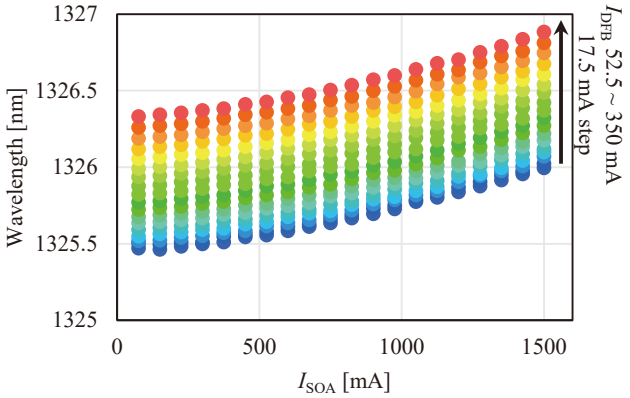

Fig. 6. I_{SOA}/I_{DFB} current dependence of oscillation spectrum transition

3-3 Relative intensity noise (RIN)

In addition to the oscillation spectrum, relative intensity noise (RIN)*5 is another essential parameter to be confirmed when considering optical communications applications. Figure 7 shows the dependence of RIN on I_{SOA} and I_{DFB} currents at T_c: 45°C. RIN mainly depends on I_{DFB}, and the average RIN decreases as I_{DFB} increases. No change

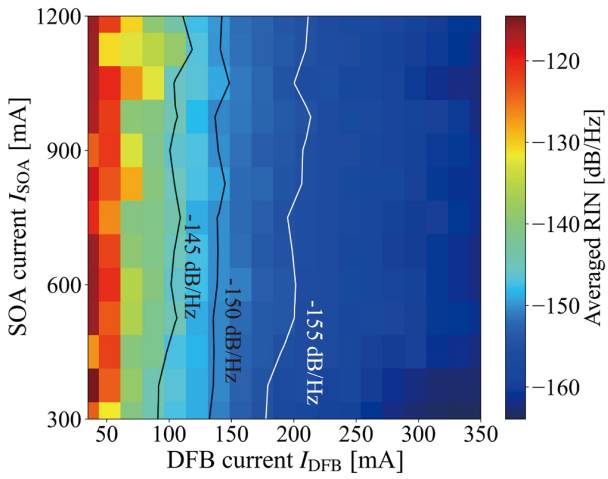

Fig. 7. I_{DFB}/I_{SOA} dependence of relative intensity noise (RIN)

trend can be observed with an increase in I_{SOA}, and low RIN below -155 dB/Hz can be obtained by operating I_{DFB} at about 200 mA or more.

3-4 Far-field pattern (FFP)

A concern when using wide-stripe waveguides is the effect on the far-field pattern (FFP)*6. High output LDs using wide-stripe waveguides can cause abnormalities such as two-peak beam shapes due to multimode oscillation[7] or a phenomenon called filamentation[12]. Figure 8 shows the measured FFP. An FFP that approximates a Gaussian shape in both horizontal and vertical directions was obtained, and the full width at half maximum (FWHM) in the horizontal and vertical directions was 12.7° and 23.2°, respectively, confirming the expected beam shape obtained from the single-mode propagation conditions.

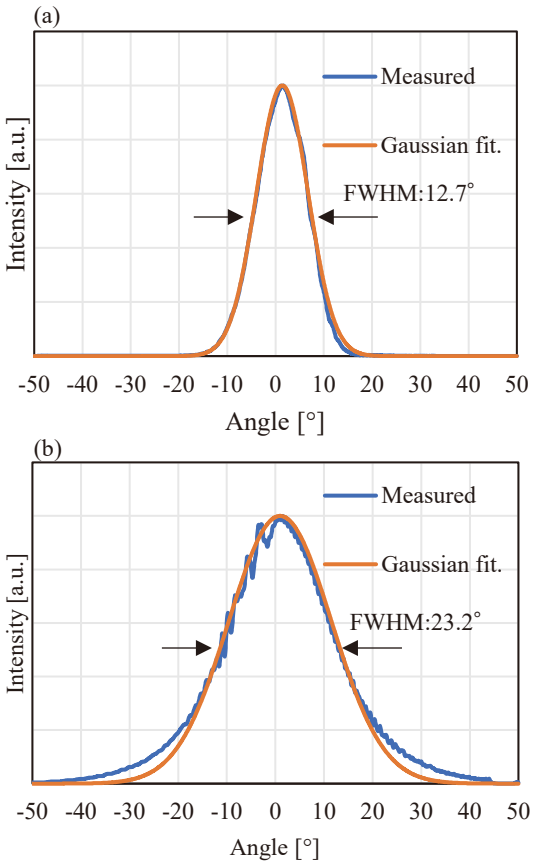

Fig. 8. FFP measurement results
(a) Horizontal direction (b) Vertical direction

4. Conclusion

We have developed a 1.3 μm band semiconductor laser with 400 mW+ light output and a high PCE of 25% at 45°C operation as a high power LD for CPO applications using the wide-stripe SOA integrated DFB-LD structure. This high power LD features high stability in the oscillation spectrum, with an SMSR of over 45dB and a low RIN of under -155 dB/Hz, proving suitable for CPO applications.

Technical Terms

∗1 Distributed feedback laser diode (DFB-LD): A semiconductor laser that allows wavelength selection by Bragg reflection through the provision of distributed grating in the laser resonator.

∗2 Semiconductor optical amplifier (SOA): A semiconductor waveguide composed of a gain medium. It allows light amplification by induced emission by injecting current and inputting light under an inverted distribution state of electrons.

∗3 Side-mode suppression ratio (SMSR): The intensity ratio of the main oscillation spectrum peak to the sideband spectrum peak.

∗4 Amplified spontaneous emission (ASE): Incoherent light that has amplified the spontaneous emission light.

∗5 Relative intensity noise (RIN): The intensity ratio of optical power noise per unit frequency to the optical power of the carrier wave.

∗6 Far-field pattern (FFP): The intensity distribution with respect to the angle of the light power emitted from the output facet of the laser.

References

(1) J. E. Johnson et al., "Performance and Reliability of Advanced CW Lasers for Silicon Photonics Applications," OFC, San Diego, CA, USA, pp. 1-27 (2022)
(2) R. Mahajan et al., "Co-Packaged Photonics For High Performance Computing: Status, Challenges And Opportunities," J. Light. Technol., 40(2), pp. 379-392 (2022)
(3) B. J. Lee et al., "Beyond CPO:A Motivation and Approach for Bringing Optics Onto the Silicon Interposer," J. Light. Technol., 41(4), 1152-1162 (2023)
(4) W. Zhou et al., "High power CW laser for co-packaged optics," CLEO, paper SS2D.3 (2022)
(5) H. Grant et al., "High-power, high-temperature O-band DFBs and SOAs for integrated photonic applications," Proc. of SPIE, PC12004 (2022)
(6) S. Yokokawa et al., "Over 100 mW Uncooled Operation of SOA-integrated 1.3−μm Highly Reliable CW-DFB Laser," OFC, San Diego, CA, USA, pp. 1-3 (2022)
(7) Y. Yamagata et al., "915nm high power broad area laser diodes with ultra-small optical confinement based on Asymmetric Decoupled Confinement Heterostructure (ADCH)" SPIE, 9348, 119-128 (2015)
(8) Dutta N.K. and Wang Q., Semiconductor Optical Amplifiers, Singapore: World Scientific; 2006
(9) A. Champagne et al., "Degradation of side-mode suppression ratio in a DFB laser integrated with a semiconductor optical amplifier," J. Quantum Electron., 40(7), 871-877 (2004)
(10) Ohtsubo J., Semiconductor laser: Stability, Instability and Chaos, New York: Springer Verlag; 2008
(11) M. R. Alalusi and R. B. Darling, "Effects of nonlinear gain on mode-hopping in semiconductor laser diodes," J. Quantum Electron, 31(7), 1181-1192 (1995)
(12) I. FISCHER et al., "Complex spatio-temporal dynamics in the near-field of a broad-area semiconductor laser." Europhysics Let., 35 (8), 579 (1996)

Contributors

The lead author is indicated by an asterisk (*).

K. AOYAMA*
• Ph.D.
Sumitomo Electric Device Innovations, Inc.

D. INOUE
• Ph.D.
Transmission Device Laboratory

N. FUJIWARA
• Ph.D.
Group Manager, Transmission Device Laboratory

H. KAMISUGI
• Manager, Sumitomo Electric Device Innovations, Inc.

D. SHOJI
• Ph.D.
Manager, Sumitomo Electric Device Innovations, Inc.